Inorg. Chem. **2007**, *46*, 1135–1143

In Situ Solvothermal Generation of 1,2,4-Triazolates and Related Compounds from Organonitrile and Hydrazine Hydrate: A Mechanism Study

Lin Cheng, Wei-Xiong Zhang, Bao-Hui Ye,* Jian-Bin Lin, and Xiao-Ming Chen*

MOE Key Laboratory of Bioinorganic and Synthetic Chemistry, School of Chemistry and Chemical Engineering, Sun Yat-Sen University, Guangzhou 510275, China

Received July 14, 2006

The facile and effective one-pot solvothermal syntheses of 3,5-disubstituted 1,2,4-triazole and its derivatives (substituted group = alkyl, aryl, and pyridyl) through cyclocondensations of organonitriles and hydrazine hydrate in the absence/presence of metal salts have been established. By control of the solvothermal conditions and/or the addition of counteranions, different intermediates and final products were derived from various organonitriles, in which an intermediate *N,N′*-bis(picolinamide)azine (H_4bpa) has been successfully trapped in its neutral manganese(II) complexes. A systematical study shows that, after the initial formation of 2-pyridylamidrazone from 2-cyanopyridine and hydrazine, two reaction paths are involved in the formation of 1,2,4-triazoles: via the formation of 3,6-bis(2-pyridyl)-1,2-dihydro-1,2,4,5-tetrazine and H_4bpa as intermediates. The tetrazine and H_4bpa paths are preferred in the absence and presence of metal ions, respectively. In the presence of metal ions, metal ion binding can stabilize the tautomers, enhance the nucleophilic reactivity of the imino C atom, and inhibit the tautomerization of H_4bpa, hence leading to the formation of 1,2,4-triazolates or H_4bpa in complexed forms. The in situ cyclocondensation reactions of 2-pyridylamidrazone and carboxylate into asymmetric 3,5-disubstituted 1,2,4-triazolates under solvothermal conditions have also been observed for the first time. Crystal structures of the crystalline metal complexes have been obtained, including dinuclear $[Mn_2(bpt)_2Cl_2(H_2O)_2]$ (**1**) and $[Mn_2(bpt)_2(SCN)_2(H_2O)_2]$ (**3**; Hbpt = 3,5-bis(2-pyridyl)-4*H*-1,2,4-triazole), tetranuclear $[Mn_4(H_3bpa)_2(mpt)_4(N_3)_2]\cdot 2H_2O$ (**5**; Hmpt = 3-methyl-5-(2-pyridyl)-1*H*-1,2,4-triazole), $[Mn_4(H_3bpa)_2(pt)_4(N_3)_2]\cdot 2C_2H_5OH$ (**6**; Hpt = 5-(2-pyridyl)-1*H*-1,2,4-triazole), and $[Mn_4(H_3bpa)_4(SCN)_4]\cdot 2C_2H_5OH$ (**7**), as well as helical [Cu(bpt)] (**2**). Among them, **7** is the first example of a neutral tetranuclear [2 × 2] grid manganese(II) complex. Both **5** and **7** exhibit antiferromagnetic interactions.

Introduction

Solvothermal (including hydrothermal hereafter) conditions have been widely used in the synthesis of inorganic materials for 6 decades.[1] During the past decade, this powerful technique has been widely used for the preparation of inorganic−organic hybrid materials and coordination polymers.[2] Some unexpected and important in situ ligand reactions were observed.[3−6] The relatively high temperatures and pressures, as well as the presence of metal ions, may facilitate some new reactions or provide facile one-pot syntheses for intriguing organic compounds that otherwise require multistep processes.[3−11] Therefore, such in situ ligand reactions are very promising as a bridge between coordina-

* To whom correspondence should be addressed. E-mail: cesybh@mail.sysu.edu.cn (B.-H.Y.), cxm@mail.sysu.edu.cn (X.-M.C.). Fax: int. code +86 20 8411-2245.

(1) For recent reviews, see: (a) Feng, S. H.; Xu, R. R. *Acc. Chem. Res.* **2001**, *34*, 239−247. (b) Cundy, C. S.; Cox, P. A. *Chem. Rev.* **2003**, *103*, 663−701. (c) Katritzky, A. R.; Nichols, D. A.; Siskin, M.; Murugan, R.; Balasubramanian, M. *Chem. Rev.* **2001**, *101*, 837−892.

(2) For recent reviews, see: (a) Evans, O. R.; Lin, W.-B. *Acc. Chem. Rev.* **2002**, *35*, 511−522. (b) Lu, J. Y. *Coord. Chem. Rev.* **2003**, *246*, 327−347. (c) Chen, X.-M.; Tong, M.-L. *Acc. Chem. Res.* **2006**, AR068084P, in press.

(3) Hu, S.; Chen, J.-C.; Tong, M.-L.; Wang, B.; Yan, Y.-X.; Batten, S.-R. *Angew. Chem., Int. Ed.* **2005**, *44*, 5471−5475.

(4) (a) Zhang, J.-P.; Zheng, S.-L.; Huang, X.-C.; Chen, X.-M. *Angew. Chem., Int. Ed.* **2004**, *43*, 206−209. (b) Zhang, X.-M.; Tong, M.-L.; Chen, X.-M. *Angew. Chem., Int. Ed.* **2002**, *41*, 1029−1031. (c) Zhang, X.-M.; Tong, M.-L.; Gong, M.-L.; Lee, H.-K.; Luo, L.; Li, K.-F.; Tong, Y.-X.; Chen, X.-M. *Chem.−Eur. J.* **2002**, *8*, 3187−3194.

(5) (a) Liu, C.-M.; Gao, S.; Kou, H.-Z. *Chem. Commun.* **2001**, 1670−1671. (b) Wang, R.-H.; Hong, M.-C.; Luo, J.-H.; Cao, R.; Weng, J.-B. *Chem. Commun.* **2003**, 1018−1019.

(6) (a) Zhang, X.-M.; Hou, J.-J.; Wu, H.-S. *Dalton Trans.* **2004**, 3437−3439. (b) Zhang, X.-M. *Coord. Chem. Rev.* **2005**, *249*, 1201−1219.

10.1021/ic061303i CCC: $37.00
Published on Web 01/13/2007

Scheme 1. In Situ Solvothermal Ligand Reactions of Organonitriles with Ammonia (a), Hydrazine (b), and Azide (c) in the Presence of Metal Ions

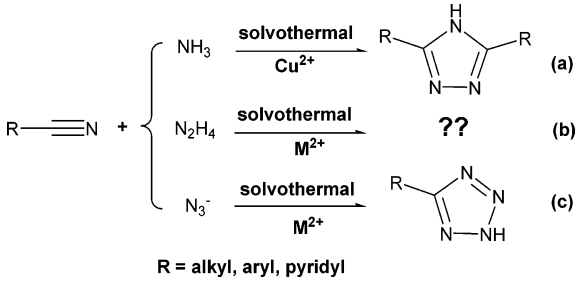

tion and synthetic organic chemistry.[3c] In contrast to the well-investigated metal−ligand reactions in conventional solution methods,[12,13] the often complicated courses involved in the organic reactions are seldom "seen" in the black-box-like solvothermal reactions. It is currently a challenge to probe the reaction mechanism of a complicated or multistep ligand reaction under solvothermal conditions.[3c,14a]

To reduce the difficulty in the mechanistic investigation of in situ solvothermal ligand reactions, it is very important to select appropriate starting reagents and reaction conditions to allow isolation of key intermediates. As illustrated in our recent study on the one-pot solvothermal treatments of organonitriles and ammonia involving copper(II) salts to yield copper(I) and corresponding 3,5-disubstituted 1,2,4-triazolates (Scheme 1a), the important intermediates and byproducts could be trapped and isolated by controlling the reaction and crystallization conditions.[14a]

Organonitriles are active for the addition reactions of nucleophiles, electrophiles, or asymmetric dipolar cycloadditions to the C≡N triple bonds,[13] offering attractive potential routes for the creation of new C−C, C−N, C−O, and C−S bonds under solvothermal conditions. In addition to the aforementioned solvothermal synthesis of 3,5-disubstituted 1,2,4-triazolates, the [2 + 3] cycloadditions of organonitriles and azides involving metal centers under solvothermal conditions afford corresponding tetrazolate coordination polymers (Scheme 1c).[15]

We report herein the in situ reactions of organonitriles with hydrazine hydrate in the presence/absence of metal ions under solvothermal conditions (Scheme 1b). On the basis of a number of intermediates and final organic ligands isolated in crystalline form, possible reaction mechanisms are discussed. Because some of the products are tetranuclear manganese(II) complexes, their magnetic properties are also reported.

Experimental Section

Materials and Physical Measurements. The reagents and solvents employed were commercially available and used as received without further purification. The C, H, and N microanalyses were carried out with a Vario EL elemental analyzer. The Fourier transform (FT)-IR spectra were recorded from KBr pellets in the range of 400−4000 cm^{-1} on a Bruker TENSOR 27 FT-IR spectrometer. The NMR spectra were recorded on a Varian 300 or 500 MHz spectrometer at 25 °C using solvent as an internal standard. The chemical shifts are reported with respect to tetramethylsilane. The mass spectra (MS) of fast atom bombardment (FAB)-MS, electron impact (EI)-MS, and electrospray ionization (ESI)-MS were obtained on VG ZAB-HS, Thermo DSQ, and Thermo Finigan LCQ DECA XP mass spectrometers, respectively. The magnetic susceptibility data of powder samples were collected in the temperature range of 2−320 K with a Quantum Design MPMS XL-7 SQUID magnetometer. The diamagnetic corrections were estimated from Pascal's constants.[16] The effective magnetic moments were calculated from the equation $\mu_{eff} = 2.828(\chi_M T)^{1/2}$.

2-Pyridylamidrazone (2-pa),[17] *N*,*N*′-bis(picolinamide)azine (H_4bpa),[18] 3,6-bis(2-pyridyl)-1,2-dihydro-1,2,4,5-tetrazine (bpdt),[19] and $Mn(HCO_2)_2{\cdot}2H_2O$[20] were synthesized in accordance with the published procedures and checked with NMR spectra or elemental analysis.

(7) (a) Tao, J.; Zhang, Y.; Tong, M.-L.; Chen, X.-M., Yuen, T.; Lin, C.-L.; Huang, X.-Y.; Li, J. *Chem. Commun.* **2002**, 1342−1343. (b) Zhang, X.-M.; Wu, H.-S.; Chen, X.-M. *Eur. J. Inorg. Chem.* **2003**, 2959−2964. (c) Huang, X.-C.; Zheng, S.-L.; Zhang, J.-P.; Chen, X.-M. *Eur. J. Inorg. Chem.* **2004**, 1024−1029. (d) Wang, Y.-T.; Fan, H.-H.; Wang, H.-Z.; Chen, X.-M. *Inorg. Chem.* **2005**, *44*, 4148−4149.

(8) (a) Zheng, Y.-Z.; Tong, M.-L.; Chen, X.-M. *New J. Chem.* **2004**, *28*, 1412−1415. (b) Han, Z.-B.; Cheng, X.-N.; Li, X.-F.; Yu, X.-L.; Chen, X.-M. *Z. Anorg. Allg. Chem.* **2005**, *631*, 937−942.

(9) (a) Li, D.; Wu, T.; Zhou, X.-P.; Zhou, R.; Huang, X.-C. *Angew. Chem., Int. Ed.* **2005**, *44*, 4175−4178. (b) Li, D.; Wu, T. *Inorg. Chem.* **2005**, *44*, 1175−1177.

(10) Cheng J.-K.; Yao, Y.-G.; Zhang, J.; Li, Z.-J.; Cai, Z.-W.; Zhang, X.-Y.; Chen, Z.-N.; Chen, Y.-B.; Kang, Y.; Qin, Y.-Y.; Wen, Y.-H. *J. Am. Chem. Soc.* **2004**, *126*, 7796−7797.

(11) Zhang, X.-M.; Fang, R.-Q.; Wu, H.-S. *J. Am. Chem. Soc.* **2005**, *127*, 7670−7671.

(12) Constable, E. C. *Metals and Ligand Reactivity*; VCH: Weinheim, Germany, 1996.

(13) (a) Michelin, R. A.; Mozzon, M.; Bertani, R. *Coord. Chem. Rev.* **1996**, *147*, 299−338. (b) Kukushkin, V. Y.; Pombeiro, A. J. L. *Chem. Rev.* **2002**, *102*, 1771−1802.

(14) (a) Zhang, J.-P.; Lin, Y.-Y.; Huang, X.-C.; Chen, X.-M. *J. Am. Chem. Soc.* **2005**, *127*, 5495−5506. (b) Zhang, J.-P.; Lin, Y.-Y.; Huang, X.-C.; Chen, X.-M. *Chem. Commun.* **2005**, 1258−1260.

(15) (a) Xiong, R.-G.; Xue, X.; Zhao, H.; You, X.-Z.; Abrahams, B. F.; Xue, Z.-L. *Angew. Chem., Int. Ed.* **2002**, *41*, 3800−3803. (b) Wang, L.-Z.; Qu, Z.-R.; Zhao, H.; Wang, X.-S.; Xiong, R.-G.; Xue, Z. *Inorg. Chem.* **2003**, *42*, 3969−3971. (c) Qu, Z.-R.; Zhao, H.; Wang, X.-S.; Li, Y.-H.; Song, Y.-M.; Liu, Y.-J.; Ye, Q.; Xiong, R.-G.; Abrahams, B. F.; Xue, Z.-L.; You, X.-Z. *Inorg. Chem.* **2003**, *42*, 7710−7712. (d) Tao, J.; Ma, Z.-J.; Huang, R.-B.; Zheng, L.-S. *Inorg. Chem.* **2004**, *43*, 6133−6135. (e) Jiang, C.; Yu, Z.; Wang, S.; Jiao, C.; Li, J.; Wang, Z.; Cui, Y. *Eur. J. Inorg. Chem.* **2004**, 3662−3667. (f) Wu, T.; Yi, B.-H.; Li, D. *Inorg. Chem.* **2005**, *44*, 4130−4132. (g) Lin, P.; Clegg, W.; Harrington, R. W.; Henderson, R. A. *Dalton Trans.* **2005**, 2388−2394. (h) Wang, X.-S.; Tang, Y.-Z.; Huang, X.-F.; Qu, Z.-R.; Che, C.-M.; Chan, P. W. H.; Xiong, R.-G. *Inorg. Chem.* **2005**, *44*, 5278−5285. (i) Ye, Q.; Li, Y.-H.; Song, Y.-M.; Huang, X.-F.; Xiong, R.-G.; Xue, Z.-L. *Inorg. Chem.* **2005**, *44*, 3618−3625. (j) Ye, Q.; Song, Y.-M.; Wang, G.-X.; Chen, K.; Fu, D.-W.; Chan, P. W. H.; Zhu, J.-S.; Huang, S. P. D.; Xiong, R.-G. *J. Am. Chem. Soc.* **2006**, *128*, 6554−6555.

(16) Kahn, O. *Molecular Magnetism*; VCH: New York, 1993.

(17) Case, F. H. *J. Org. Chem.* **1965**, *30*, 931−933.

(18) Xu, Z.; Thompson, L. K.; Miller, D. O. *Inorg. Chem.* **1997**, *36*, 3985−3995. For H_4bpa. Anal. Calcd (%) for $C_{12}H_{12}N_6$: C, 59.99; H, 5.03; N, 34.98. Found: C, 59.94; H, 4.45; N, 34.78. IR (KBr, ν/cm^{-1}): 3464.2vs, 3275.6w, 1610.7vs, 1559.8vs, 1465.7vs, 1375.6s, 799.3vs, 746.7vs, 672.1s. ^{1}H NMR (CD_3OD): δ 8.58 (d, J = 3.0 Hz, 2H), 8.34 (d, J = 5.1 Hz, 2H), 7.84 (t, 2H), 7.41 (t, 2H) ppm. ^{13}C NMR (CD_3OD): δ 153.2, 150.8, 148.2, 136.0, 124.3, 120.7 ppm. EI-MS: m/z 240 $[M]^+$.

(19) Geldard, J. F.; Lions, F. *J. Org. Chem.* **1965**, *30*, 318−319. For bpdt. Anal. Calcd (%) for $C_{12}H_{10}N_6$: C, 60.50; H, 4.23; N, 35.27. Found: C, 60.21; H, 4.45; N, 35.05. IR (KBr, ν/cm^{-1}): 3341.6vs, 3296.0vs, 1588.2s, 1446.4vs, 1386.0vs, 1115.8s, 978.1s, 884.1s, 791.2s. ^{1}H NMR (CD_3OD): δ 8.50−8.58 (m, 4H), 8.03 (d, J = 8 Hz, 2H), 7.84 (t, 2H), 7.41 (t, 2H) ppm. ^{13}C NMR (CD_3OD): δ 148.2, 147.3, 146.5, 136.6, 124.8, 121.2 ppm. EI-MS: m/z 238 $[M]^+$.

(20) Kazuo, Y. *J. Phys. Soc. Jpn.* **1967**, *22*, 582−589.

Abbreviations of the other organic ligands/compounds: admt = 4-amino-3,5-dimethyl-1,2,4-triazole; adpt = 4-amino-3,5-diphenyl-1,2,4-triazole; 2-abpt = 4-amino-3,5-bis(2-pyridyl)-1,2,4-triazole; 3-abpt = 4-amino-3,5-bis(3-pyridyl)-1,2,4-triazole.

Synthesis of admt, adpt, 2-abpt, and 3-abpt in the Absence of Metal Salts. A mixture of organonitrile (25 mmol), $NH_2NH_2 \cdot H_2O$ (80%, 3 mL), and anhydrous ethanol (1 mL) was heated in a 15 mL Teflon-lined autoclave at 120 °C for 3 days, followed by slow cooling (5 °C h^{-1}) to room temperature. The resulting colorless block crystals were collected by filtration. The filtered solution was further evaporated, and more colorless powder was obtained. All solid products were collected and then dried.

The yield of admt was ca. 84%. Anal. Calcd (%) for $C_4H_8N_4$: C, 42.85; H, 7.19; N, 49.96. Found: C, 42.88; H, 7.20; N 49.93. IR: 3245s, 3152s, 3007m, 2362m, 1651vs, 1538s, 1423vs, 1353vs, 1259m, 1091m, 1049w, 991vs, 761m, 743w, 662m, 511m, 479m cm^{-1}. ESI-MS: *m*/*z* 113 $[M + H]^+$. ^1H NMR (CD_3OD, ppm): δ 2.38 (s, 6H, CH_3), 4.94 (s, 2H, NH_2).

The yield of adpt was ca. 91%. Anal. Calcd (%) for $C_{14}H_{12}N_4$: C, 71.17; H, 5.12; N, 23.71. Found: C, 71.20; H, 5.13; N, 23.68. IR: 3746w, 3427m, 3315vs, 3146s, 2362w, 1628vs, 1057s, 1458vs, 1155m, 1066m, 957m, 732s, 694s, 562m, 504m cm^{-1}. EI-MS: *m*/*z* 236 $[M]^+$. ^1H NMR (CD_3OD, ppm): δ 4.90 (s, 2H, NH_2), 7.53 (m, 4H), 7.99 (m, 6H).

The yield of 2-abpt was ca. 70%. Anal. Calcd (%) for $C_{12}H_{10}N_6$: C, 60.50; H, 4.23; N, 35.27. Found: C, 60.47; H, 4.18; N, 35.29. IR: 3854w, 3292s, 1658m, 1585s, 1464vs, 1426m, 1246w, 1146m, 1084w, 997m, 962m, 790vs, 737s, 688vs, 620m, 583m cm^{-1}. EI-MS: *m*/*z* 238 $[M]^+$. ^1H NMR (CD_3OD, ppm): δ 4.90 (s, 2H, NH_2), 7.52 (m, 2H), 8.00 (m, 2H), 8.24 (m, 2H), 8.76 (d, 2H).

The yield of 3-abpt was ca. 73%. Anal. Calcd (%) for $C_{12}H_{10}N_6$: C, 60.50; H, 4.23; N, 35.27. Found: C, 60.52; H, 4.21; N, 35.26. IR: 3751w, 3414m, 3363s, 3272vs, 3205vs, 2975m, 2367s, 1964s, 1624m, 1598vs, 1572m, 1463s, 1422vs, 1397m, 1272m, 1192m, 1137m, 1089m, 1028vs, 1006m, 967m, 905m, 813m, 709s, 617m cm^{-1}. EI-MS: *m*/*z* 238 $[M]^+$. ^1H NMR (CD_3OD, ppm): δ 4.94 (s, 2H, NH_2), 7.65 (m, 2H), 8.48 (m, 2H), 8.71 (m, 2H), 9.19 (d, 2H).

Synthesis of admt, adpt, and 3-abpt in the Presence of Metal Salts. A typical synthetic procedure is described below. A mixture of organonitrile (5 mmol), hydrazine hydrate (80%, 3 mL), and anhydrous ethanol (1 mL) was added to a 15 mL Teflon-lined autoclave and stirred for 12 h, and then a copper(II) or manganese(II) salt (1 mmol) was added to the above solution. The mixture was heated in a 15 mL Teflon-lined autoclave at 120 °C for 3 days, followed by slow cooling (5 °C h^{-1}) to room temperature. The resulting filtrate was allowed to stand at room temperature in air for a few days by slow evaporation. Colorless block crystals were collected by filtration and dried in an oven at 110 °C. The yields were ca. 50−80% based on the organonitriles.

Synthesis of $[Mn_2(bpt)_2Cl_2(H_2O)_2]$ (1). A mixture of 2-cyanopyridine (0.5 g, 4.8 mmol), hydrazine hydrate (80%, 1.5 mL), and anhydrous ethanol (2 mL) was added to a 15 mL Teflon-lined autoclave and stirred for 12 h, and then $MnCl_2 \cdot 4H_2O$ (0.198 g, 1 mmol) was added to the mixture. The autoclave was then heated in an oven at 160 °C for 3 days, followed by slow cooling to room temperature at 5 °C h^{-1}. The resulting product was filtered and washed with anhydrous ethanol, and pale-yellow crystals were collected and dried in air (ca. 6% yield based on Mn). Anal. Calcd (%) for $C_{24}H_{20}Cl_2Mn_2N_{10}O_2$: C, 43.59; H, 3.05; N, 21.18. Found: C, 43.64; H, 3.03; N, 21.20. IR: 3845w, 3745w, 3373s, 3045w, 2303w, 1670m, 1602s, 1567m, 1498m, 1466vs, 1403s, 1261w, 1252w, 1186m, 1140m, 1094m, 1014m, 802m, 752m, 727m, 634m cm^{-1}.

Synthesis of $[Cu(bpt)]_\infty$ (2). Method A. The reaction was carried out in a procedure similar to that of **1**, using $Cu(CH_3CO_2)_2 \cdot H_2O$ (0.20 g, 1 mmol) instead of $MnCl_2 \cdot 4H_2O$. The resulting product was collected by filtration, washed with anhydrous ethanol, and dried in air, giving red block crystals (ca. 56% yield based on Cu). Anal. Calcd (%) for $C_{12}H_8CuN_5$: C, 50.44; H, 2.82; N, 24.51. Found: C, 50.48; H, 2.92; N, 24.51. IR: 3854w, 3745w, 3428vs, 3055vs, 2597w, 2432w, 2342w, 2006w, 1913w, 1846w, 1599s, 1563m, 1498vs, 1426s, 1255m, 1185w, 1148m, 1093m, 1001m, 895w, 796vs, 739s, 630w, 503w cm^{-1}.

Method B. A mixture of 2-pa (0.272 g, 2 mmol), $Cu(CH_3CO_2)_2 \cdot H_2O$ (0.200 g, 1 mmol), and ethanol (95%, 4 mL) was added to a 15 mL Teflon-lined autoclave, which was then heated at 160 °C for 3 days, followed by slow cooling (5 °C h^{-1}) to room temperature. The resulting mixture was filtered and washed with 95% ethanol, and red block crystals were collected and dried in air (ca. 82% yield based on Cu). The same product (checked with the unit cell parameters) was obtained (80% based on Cu) when the temperature was set at 120 °C.

Synthesis of $[Mn_2(bpt)_2(SCN)_2(H_2O)_2]$ (3). Method A. A mixture of 2-pa (0.272 g, 2 mmol), $MnSO_4 \cdot H_2O$ (0.169 g, 1 mmol), KSCN (0.097 g, 1 mmol), and 95% ethanol (4 mL) was heated in a 15 mL Teflon-lined autoclave at 120 °C for 3 days, followed by slow cooling (5 °C h^{-1}) to room temperature. The resulting mixture was filtered and washed with 95% ethanol, and pale-yellow block crystals were collected and dried in air (ca. 35% yield based on Mn). Anal. Calcd (%) for $C_{26}H_{20}Mn_2N_{12}O_2S_2$: C, 44.20; H, 2.85; N, 23.79. Found: C, 44.21; H, 2.84; N, 23.81. IR: 3854m, 3744m, 3426s, 2060s, 1646m, 1606vs, 1562m, 1505m, 1409vs, 1113m, 1043m, 800m, 736m, 628m cm^{-1}.

Method B. The reaction was carried out in a procedure similar to that of method A, using H_4bpa (0.240 g, 1 mmol) instead of 2-pa (ca. 46% yield based on Mn).

Method C. The reaction was carried out in a procedure similar to that of method A, using bpdt (0.240 g, 1 mmol) instead of 2-pa (ca. 42% yield based on Mn).

Method D. The reaction was carried out in a procedure similar to that of method A, only using 2-abpt (1 mmol) instead of 2-pa (ca. 52% yield based on Mn).

$Zn_2(admt)_2Cl_4$ (4). A mixture of admt (0.120 g, 1 mmol), $ZnCl_2$ (0.136 g, 1 mmol), and 95% ethanol (4 mL) was heated in a 15 mL Teflon-lined autoclave at 140 °C for 3 days, followed by slow cooling (5 °C h^{-1}) to room temperature. The resulting mixture was filtered and washed with 95% ethanol, and colorless block crystals were collected and dried in air (ca. 93% yield based on Zn). Anal. Calcd (%) for $C_8H_{16}Cl_4N_8Zn_2$: C, 19.34; H, 3.25; N, 22.55. Found: C, 19.30; H, 3.27; N, 22.59. IR: 3801w, 3673w, 3649w, 3337s, 3269vs, 2938w, 1612s, 1554s, 1425m, 1393vs, 1274m, 1107m, 1043m, 1010m, 966vs, 784vs, 751m, 665m, 598s, 546m cm^{-1}.

$[Mn_4(H_3bpa)_2(mpt)_4(N_3)_2] \cdot 2H_2O$ (5; Hmpt = 3-Methyl-5-(2-pyridyl)-1*H*-1,2,4-triazole). The reaction was carried out in a procedure similar to that of method A for **3**, using $Mn(CH_3CO_2)_2 \cdot 4H_2O$ (0.245 g, 1 mmol) and NaN_3 (0.130 g, 2 mmol) instead of $MnSO_4 \cdot H_2O$ and KSCN, respectively. The resulting mixture was filtered and washed with 95% ethanol, and red block crystals were collected and dried in air (ca. 23% yield based on Mn). Anal. Calcd (%) for $C_{56}H_{54}Mn_4N_{34}O_2$: C, 46.23; H, 3.74; N, 32.73. Found: C, 46.22; H, 3.77; N, 32.71. IR: 3856m, 3744m, 3649m, 3422vs, 2920w, 2362s, 1835w, 1740m, 1698m, 1646vs, 1558m, 1514m, 1461m, 1426w, 1052w, 672m cm^{-1}.

$[Mn_4(H_3bpa)_2(pt)_4(N_3)_2]\cdot 2C_2H_5OH$ [6; Hpt = 5-(2-Pyridyl)-1*H*-1,2,4-triazole]. The reaction was carried out in a procedure similar to that for **5**, using $Mn(HCO_2)_2\cdot 2H_2O$ (0.181 g, 1 mmol) instead of $Mn(CH_3CO_2)_2\cdot 4H_2O$. The resulting mixture was filtered and washed with 95% ethanol, and red platelike crystals were collected and dried in air (ca. 20% yield based on Mn). Anal. Calcd (%) for $C_{56}H_{54}Mn_4N_{34}O_2$: C, 46.23; H, 3.74; N, 32.73. Found: C, 46.22; H, 3.77; N, 32.71. IR: 3854w, 3743m, 3440vs, 2361s, 2052s, 1648vs, 1539vs, 1468m, 1357m, 1273m, 1155m, 1109m, 1037m, 800w, 675m cm^{-1}.

$[Mn_4(H_3bpa)_4(SCN)_4]\cdot 2C_2H_5OH$ (7). A mixture of 2-pa (0.272 g, 2 mmol), $Mn(CH_3CO_2)_2\cdot 4H_2O$ (0.245 g, 1 mmol), KSCN (0.085 g, 1 mmol), and C_2H_5OH (95%, 4 mL) was heated in a 15 mL Teflon-lined autoclave at 120 °C for 3 days, followed by closing of the oven and direct cooling to room temperature. The resulting mixture was filtered and washed with 95% ethanol, and red block crystals were collected and dried in air (ca. 54% yield based on Mn). Anal. Calcd (%) for $C_{56}H_{56}N_{28}Mn_4O_2S_4$: C, 44.80; H, 3.76; N, 26.12. Found: C, 44.85; H, 3.80; N, 26.08. IR: 3446s, 3338s, 2974w, 2362w, 2065s, 1650s, 1598m, 1543s, 1474vs, 1437vs, 1416m, 1353m, 1295vs, 1165w, 1090s, 1047m, 880w, 791w, 741m, 711m, 673m, 635m cm^{-1}. FAB-MS: *m*/*z* 1353 $[Mn_4(H_3bpa)_4(SCN)_3]$, 1293 $[Mn_4(H_3bpa)_4(SCN)_2]$, 1236 $[Mn_4(H_3bpa)_4(SCN)]$, 1176 $[Mn_4(H_3bpa)_4]$.

X-ray Crystallography. Diffraction intensities for all of the compounds were collected on a Bruker Apex CCD diffractometer (Mo Kα, λ = 0.710 73 Å). Absorption corrections were applied by using the multiscan propram *SADABS*.[21] The structures were solved by direct methods and refined with a full-matrix least-squares technique with the *SHELXTL* program package.[22] Anisotropic thermal parameters were applied to all the non-H atoms. The organic H atoms were generated geometrically (C−H 0.96 Å); the H atoms of aqua, hydroxyl, and amido groups were located from difference maps and refined with isotropic temperature factors. Crystal data as well as details of data collection and refinements for the complexes are summarized in Table 1.

Table 1. Crystallographic Data and Structural Refinements

compound	**1**	**2**	**3**
formula	$C_{24}H_{20}Cl_2Mn_2N_{10}O_2$	$C_{12}H_8CuN_5$	$C_{26}H_{20}Mn_2N_{12}O_2S_2$
fw	661.27	285.78	706.54
space group	$C222_1$	$P4_12_12$	$C2/c$
a/Å	12.7851(17)	11.496(1)	27.612(3)
b/Å	15.0878(19)	11.496(1)	7.5526(9)
c/Å	27.705(4)	18.224(4)	15.006(2)
β/deg	90	90	107.841(2)
V/Å^3	5344.3(12)	2408.8(6)	2978.9(6)
Z	8	8	4
D_c/g cm^{-3}	1.644	1.576	1.575
T/K	293(2)	293(2)	293(2)
μ/mm^{-1}	1.189	1.800	1.036
R1[a] ($I > 2\sigma$)	0.0713	0.0673	0.0516
wR2[a] (all data)	0.1296	0.1395	0.1218
GOF	0.969	1.079	1.079
compound	**5**	**6**	**7**
formula	$C_{56}H_{54}Mn_4N_{34}O_2$	$C_{56}H_{54}Mn_4N_{34}O_2$	$C_{56}H_{56}Mn_4N_{28}O_2S_4$
fw	1455.09	1455.09	1501.33
space group	$P2_1/c$	$P2_1/c$	$C2/c$
a/Å	12.4385(11)	13.0013(7)	25.738(2)
b/Å	16.8446(15)	13.2584(7)	14.987(1)
c/Å	18.7956(13)	19.6224(8)	18.876(2)
β/deg	131.062(4)	111.617(3)	121.038(2)
V/Å^3	2969.3(5)	3144.5(3)	6238.6(10)
Z	2	2	4
D_c/g cm^{-3}	1.627	1.537	1.598
T/K	293(2)	120(2)	293(2)
μ/mm^{-1}	0.909	0.858	0.994
R1[a] ($I > 2\sigma$)	0.0654	0.0581	0.0694
wR2[a] (all data)	0.1842	0.1647	0.1903
GOF	1.039	1.089	1.024

[a] $R1 = \sum||F_o| - |F_c||/\sum|F_o|$. $wR2 = [\sum w(F_o^2 - F_c^2)^2/\sum w(F_o^2)^2]^{1/2}$.

Results and Discussion

Syntheses, Reaction Mechanisms, and Structures. Because the 2-pyridyl group may coordinate to metal ions and assist the stabilization and trapping of the intermediates in complexed forms, we initially chose 2-cyanopyridine to react with hydrazine hydrate in the presence of metal salts under solvothermal conditions. Fortunately, 2-cyanopyridine did react with hydrazine hydrate in the presence of $MnCl_2$ to yield **1** containing the in situ generated bpt ligand.

As shown in Figure 1, there are three crystallographically independent Mn^{II} ions in two dinuclear isomers in **1**. Each Mn^{II} ion adopts a distorted octahedral coordination geometry, being chelated by two tetradentate bpt ligands in the cis bischelate fashion at the equatorial plane. Among them, Mn1 is further ligated by two aqua molecules, while each of Mn2 and Mn3 is coordinated by two chloride ions and by an aqua molecule and a chloride ion at the axial positions, respectively. The intradimer distances of Mn1···Mn2 and Mn3···Mn3b are 4.541 and 4.547 Å, respectively.

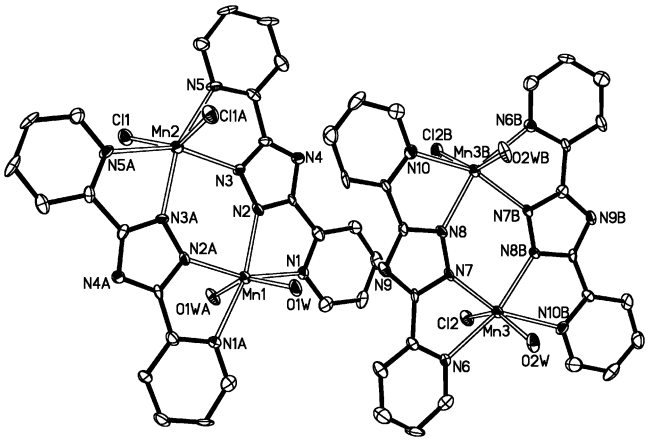

Figure 1. ORTEP plot of the dinuclear isomers in **1** (thermal ellipsoids, 30%; H atoms are omitted for clarity; A, $-x$, y, $^5/_2 - z$; B, x, $2 - y$, $2 - z$). Selected interatomic distances (Å): Mn1−O1w 2.207(6), Mn1−N1 2.303(8), Mn1−N2 2.173(6), Mn2−Cl1 2.500(2), Mn2−N3 2.216(6), Mn2−N5 2.381(8), Mn3−N6 2.338(6), Mn3−N7 2.209(6), Mn3−N8B 2.208(5), Mn3−N10B 2.343(6), Mn3−Cl2 2.471(2), Mn3−O2w 2.236(5) Å; Mn1···Mn2 4.541, Mn3···Mn3B 4.547.

To compare with our previous report on the reactions of organonitriles and ammonia in the presence of a copper(II) salt, a copper(II) salt was also employed instead of manganese(II). Indeed, **2** was obtained in a much higher yield of 56%,[14b] which has the same formula as that (referred to as **2′**) synthesized by the in situ generation with organonitriles and ammonia in the presence of Cu^{II}. **2** crystallizes in the chiral space group $P4_12_12$, and the crystal used in the diffraction happened to be an enantiomer of the crystal reported for **2′** (crystallized in space group $P4_32_12$).[14b] Similar to **2′**, the in situ synthesized bpt ligand acts in the tetradentate mode in **2**, bridging the tetrahedral Cu^I ions in the trans bis-

(21) Sheldrick, G. M. *SADABS*, version 2.05; University of Göttingen: Göttingen, Germany, 2002.
(22) *SHELXTL*, version 6.10; Bruker Analytical Instrumentation: Madison, WI, 2000.

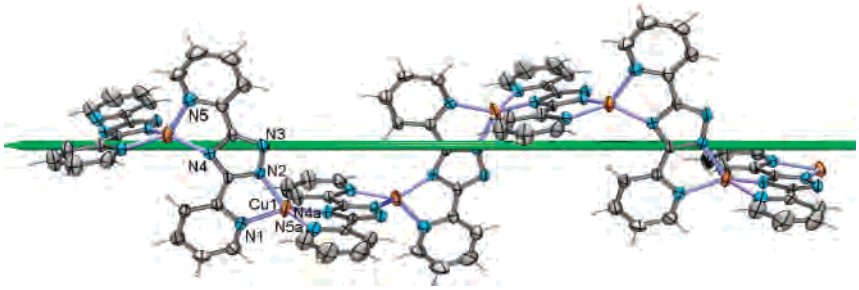

Figure 2. ORTEP drawing of a single 4_1 helix in **2** (thermal ellipsoids, 30%; a, $^3/_2 - y$, $-^1/_2 + x$, $^1/_4 + z$).

Scheme 2. Possible Formation Mechanisms of 1,2,4-Triazoles from Organonitriles and Hydrazine in the Absence of Metal Ions

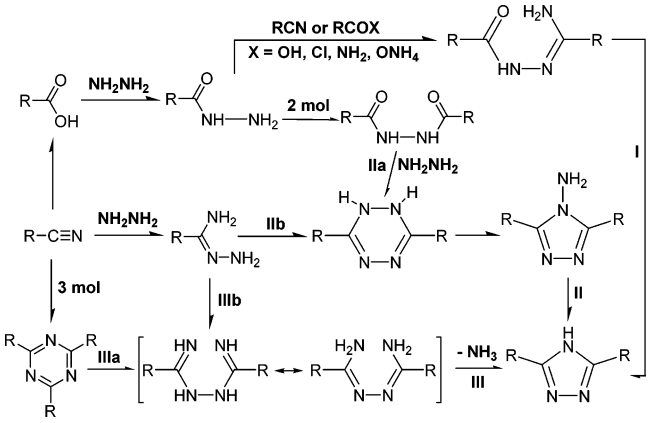

chelate fashion into a one-dimensional chain running along the crystallographic 4_1-screw axis (Figure 2). The Cu^I ions arise from excess hydrazine reduction of Cu^{II}, and the relatively high yield of **2** can be attributed to the easier crystallization nature of the infinite polymer.

So far, no one-pot synthesis of 1,2,4-triazoles from organonitrile with hydrazine hydrate has been reported. In contrast, they were synthesized by multistep reactions or from other noncommercial reagents as starting materials, as shown in Scheme 2.[19,23−29] Compared with the classical method, our approach is a facile, one-pot generation in good yield from commercially available organonitrile and hydrazine hydrate (Scheme 3).

To further explore the reaction mechanism, ESI-MS spectra of the filtrate in the synthesis of **1** were recorded, showing signals at *m*/*z* 222 and 239 (negative charge) and at *m*/*z* 224 and 239 (positive charge),[30] respectively. The data indicate that H_4bpa (239, $[M - H]^-$) and bpdt and/or 2-abpt

Scheme 3. One-Pot Solvothermal Generation of a 3,5-Bis(2-pyridyl)-1,2,4-triazolate (bpt) Anion

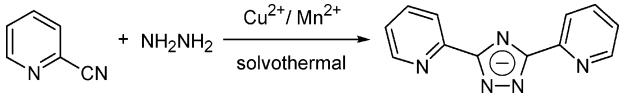

(239, $[M + H]^+$) may be the intermediates in the formation of Hbpt (222, $[M - H]^-$; 224, $[M + H]^+$). On the other hand, because H_4bpa, bpdt, and 2-abpt can be synthesized from the same precursor 2-pa that can be easily formed by the reaction of 2-cyanopyridine and hydrazine hydrate at room temperature,[17] 2-pa may be a key intermediate. To further verify this deduction, 2-pa was directly employed as the starting material to react with $Cu(CH_3CO_2)_2$ at 160 and 120 °C, giving **2** in good yield up to 82% and 80%, respectively. Moreover, when the manganese(II) salt was used in place of $Cu(CH_3CO_2)_2$ to react with 2-pa, C_2-symmetrically dimeric **3** was isolated in a higher yield. The bpt ligand in **3** acts in a cis bis-chelate fashion to ligate two Mn^{II} ions, and each Mn^{II} is further ligated by a thiocyanide-*N* and an aqua ligand to furnish a distorted octahedral geometry, as shown in Figure 3.

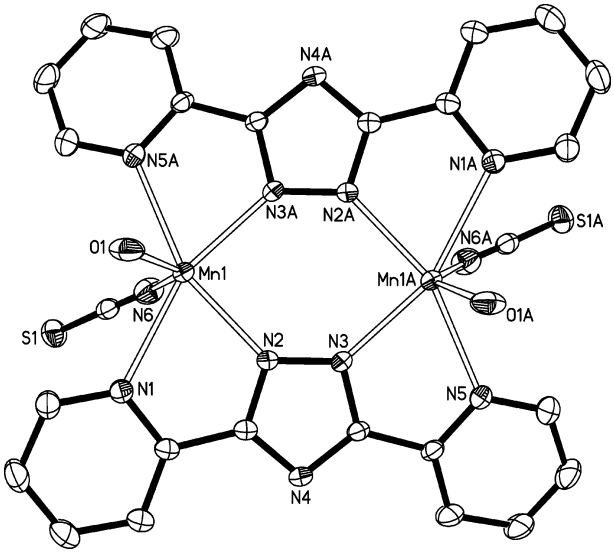

Figure 3. ORTEP plot of **3** (thermal ellipsoids, 30%; H atoms are omitted for clarity; A, $1 - x, y, ^1/_2 - z$). Selected interatomic distances (Å): Mn1−O1 2.139(3), Mn1−N1 2.426(3), Mn1−N2 2.210(2), Mn1−N6 2.134(3), Mn1−N3A 2.208(3), Mn1−N5A 2.396(3), Mn1···Mn1A 4.51.

The above observation suggests that 2-pa is a real intermediate for the generation of bpt from the organonitrile and hydrazine hydrate under solvothermal conditions in the presence of metal ions. This is in agreement with the

(23) (a) Potts, K. T. *J. Chem. Soc.* **1954**, 3461−3464. (b) Potts, K. T. *Chem. Rev.* **1960**, 87−127.
(24) Polya, J. A. In *Comprehensive Heterocyclic Chemistry*; Katritzky, A. R., Rees, C. W., Eds.; Pergamon: Oxford, U.K., 1984; Vol. 5, p 733.
(25) Garratt. P. J. In *Comprehensive Heterocyclic Chemistry II*; Katritzky, A. R., Rees, C. W., Scriven, E. F. V., Eds.; Elsevier: Oxford, U.K., 1996; Vol. 4, p 127.
(26) Curtis, A. D. M. *Sci. Synth.* **2004**, *13*, 603−639.
(27) (a) Bentiss, F.; Lagrenée, M.; Traisnel, M.; Mernari, B.; Elattari, H. *J. Heterocycl. Chem.* **1999**, *36*, 149−152. (b) Bentiss, F.; Lagrenee, M.; Barbry, D. *Tetrahedron Lett.* **2000**, *41*, 1539−1541. (c) Bentiss, F.; Lagrenee, M.; Vezin, H.; Bouanis, M.; Mernari, B. *J. Heterocycl. Chem.* **2002**, *39*, 93−96.
(28) Ikemi, Y.; Hayashi, N.; Kakehi, A.; Matsumoto, K. *Heterocycl. Commun.* **2002**, *8*, 439−442.
(29) Neilson, D. G.; Roger, R.; Heatlie, J. W. M.; Newlands, L. R. *Chem. Rev.* **1970**, *70*, 151−170.

literature reports outlined in Scheme 2. However, two possible paths, IIb and IIIb (Scheme 2), may lead to the formation of the triazolate bpt because, in using the attainable intermediates H_4bpa, bpdt, and 2-abpt as the starting materials in place of 2-pa, the same complex **3** could be obtained in yields of 46%, 42%, and 52%, respectively, in accordance with the analytical results of the filtrate from the synthesis of **1** by ESI-MS.[30]

To clarify the reaction mechanism and develop the one-pot approach to various organonitriles such as alkylnitriles, arylnitriles, and other pyridylnitriles, we performed systematic trials in the presence and absence of metal salts under solvothermal conditions. In the absence of a metal salt, acetonitrile, benzonitrile, 3-cyanopyridine, and 2-cyanopyridine reacted with hydrazine hydrate under solvothermal conditions, furnishing corresponding 4-amino-3,5-disubstituted 1,2,4-trizoles in crystalline forms with good yields and high purity. Hence, path IIb (via the formation of 3,6-disubstituted 1,2-dihydro-1,2,4,5-tetrazine) should be dominant and similar to the synthesis of aryl- or pyridyl-4-amino-1,2,4-triazoles by acid catalysis.[26] It is noteworthy that alkylnitriles are inactive in the case of acid catalysis. In the presence of a copper(II) or manganese(II) salt, acetonitrile, benzonitrile, and 3-cyanopyridine can react with hydrazine hydrate to form the corresponding 4-amino-3,5-disubstituted 1,2,4-triazoles in the crystalline forms free of metal coordination in good yields. Further experiments demonstrated that, when 2-abpt and admt reacted with metal ions in ethanol under solvothermal conditions, respectively, deaminated bpt in its metal complex **3** and intact admt (even at a higher temperature, 140 °C) in **4** (for its crystal structure, see the Supporting Information) were formed.[31] The above observations suggest that the reaction mechanism starting from 2-cyanopyridine may be different from that starting from other organonitriles in the presence of metal salts.

Obviously, as the key intermediate in the formation of 2-abpt, 2-pa has a unique chelate ability to metal ions, which is different from methyl-, phenyl-, and 3-pyridylamidrazones.[19,23−29] Though both the ESI-MS signals of bpdt/2-abpt and H_4bpa have been observed as mentioned above, this deduction still requires more experimental proof. Such proof may be obtained by tuning the reaction conditions such as the temperature, time, and solvent as well as changing the auxiliary ligands and/or counterions to control the crystallization for trapping the possible intermediates in the crystalline forms.[14a] In contrast to the direct formation of bpt in the presence of $MnCl_2$ or $Cu(CH_3CO_2)_2$ at 160 °C, when $Mn(CH_3CO_2)_2{\cdot}4H_2O$ was used and the reaction temperature was decreased to 120 °C, **5** bearing two in situ generated ligands mpt and H_3bpa in the ratio of 2:1 was isolated. The H_3bpa anion is one of the key intermediates in the formation of 3,5-disubstituted 1,2,4-trizolates (path IIIb in Scheme 2), while the asymmetrically 3,5-disubstituted mpt ligand should be generated from the reaction of 2-pa with acetate (Scheme 4).[32] Such an asymmetrically 3,5-disubstituted triazolate is unprecedented in solvo(hydro)thermal reactions but can be synthesized via cyclocondensation of the asymmetric *N*,*N*′-diamidines at high temperature (180−200 °C).[33] A parallel reaction using $Mn(HCO_2)_2{\cdot}2H_2O$ as the metal salt successfully gave **6**, in which pt in place of mpt is also an asymmetrically substituted triazolate. This fact further supports the above deduction of the cyclization of 2-pa with carboxylate.

Scheme 4. In Situ Solvothermal Generation of Asymmetrically Disubstituted 1,2,4-Triazolates

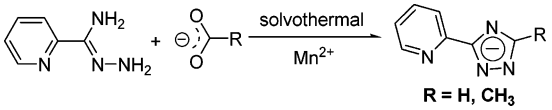

As shown in Figure 4, the structures of **5** and **6** are similar. They feature neutral, centrosymmetric, tetranuclear Mn^{II} cores ligated by two H_3bpa, four mpt (or pt), and two azide ligands, respectively, in which a pair of mpt (or pt) ligands bridge two octahedral Mn^{II} ions (Mn···Mn 4.32 or 4.28 Å) via two diazine N−N groups and each H_3bpa ligand connects to two Mn^{II} ions (separated at 4.02 or 3.91 Å) through its imino bridge to form a parallelogram. Each mpt (or pt) ligand ligates two Mn^{II} ions in a tridentate mode, while H_3bpa acts as a pentadentate ligand with a monodentate and a bridging imino group, as well as two pyridyl groups in the cis conformation. The C6−N2 bond lengths [1.283(6) Å for **5** and 1.299(5) Å for **6**] are significantly shorter than the uncoordinated C7−N5 [1.332(7) and 1.326(5) Å] and C6−N3 [1.302(9) and 1.309(5) Å] bonds. The pentadentate coordination mode for H_3bpa has not been found in the Cambridge Structural Database.[34] In contrast, neutral H_4bpa usually acts as a tetradentate ligand using two pyridyl and two imino N atoms in the trans conformation to furnish a helical structure.[35,36] The successful trapping of this unusual H_3bpa ligand can be attributed to the lower reaction temperature, as well as the introduction of azide as an auxiliary ligand to promote the crystallization of **5** and **6**.

When KSCN was used in place of NaN_3 for the generation of **6**, a tetranuclear $[Mn_4(H_3bpa)_2(pt)_4(SCN)_2]$ similar to **6** was obtained.[37] However, when KSCN was used in place of NaN_3 for the generation of **5**, neutral tetranuclear **7** was afforded in 54% yield without the presence of mpt. This fact indicates that formate may be more reactive to 2-pa to form

(30) The filtrate of the reaction solution of **1** was directly analyzed via ESI-MS. Two signals at *m*/*z* 222 and 239 were found in the negative charge detection, while *m*/*z* 224 and 239 peaks were measured in the positive charge detection (see Figure S8 in the Supporting Information).

(31) Lavrenova, L. G.; Baidina, I. A.; Ikorskii, V. N.; Sheludyakova, L. A.; Larionov, S. V. *Zh. Neorg. Khim.* **1992**, *37*, 630−636.

(32) Roppe, J.; Smith, N. D.; Huang, D.-H.; Tehrani, L.; Wang, B.-W.; Anderson, J.; Brodkin, J.; Chung, J.; Jiang, X.-H.; King, C.; Munoz, B.; Varney, M. A.; Prasit, P.; Cosford, N. D. P. *J. Med. Chem.* **2004**, *47*, 4645−4648.

(33) Kauffmann, T.; Ban, L.; Kuhlmann, D. *Chem. Ber.* **1981**, *114*, 3684−3690.

(34) Cambridge Structural Database, CCDC, Cambridge, U.K., version 5.27 (Aug 2006).

(35) Thompson, L. K. *Coord. Chem. Rev.* **2002**, *233*−*234*, 193−206.

(36) Gao, E.-Q.; Yue, Y.-F.; Bai, S.-Q.; He, Z.; Yan, C.-H. *J. Am. Chem. Soc.* **2004**, *126*, 1419−1429.

(37) X-ray diffraction shows the skeleton of the structure to be of a tetranuclear complex containing two H_3bpa, four pt, and two SCN^- ligands. Anal. Calcd (%) for $C_{54}H_{42}Mn_4N_{30}S_2$: C, 46.49; H, 3.03; N, 30.12. Found: C, 46.45; H, 3.03; N, 30.16. Space group *C*2/*c*, a = 23.424(16) Å, b = 13.587(9) Å, c = 19.147(13) Å, β = 91.51(1)° (see Figure S2 in the Supporting Information).

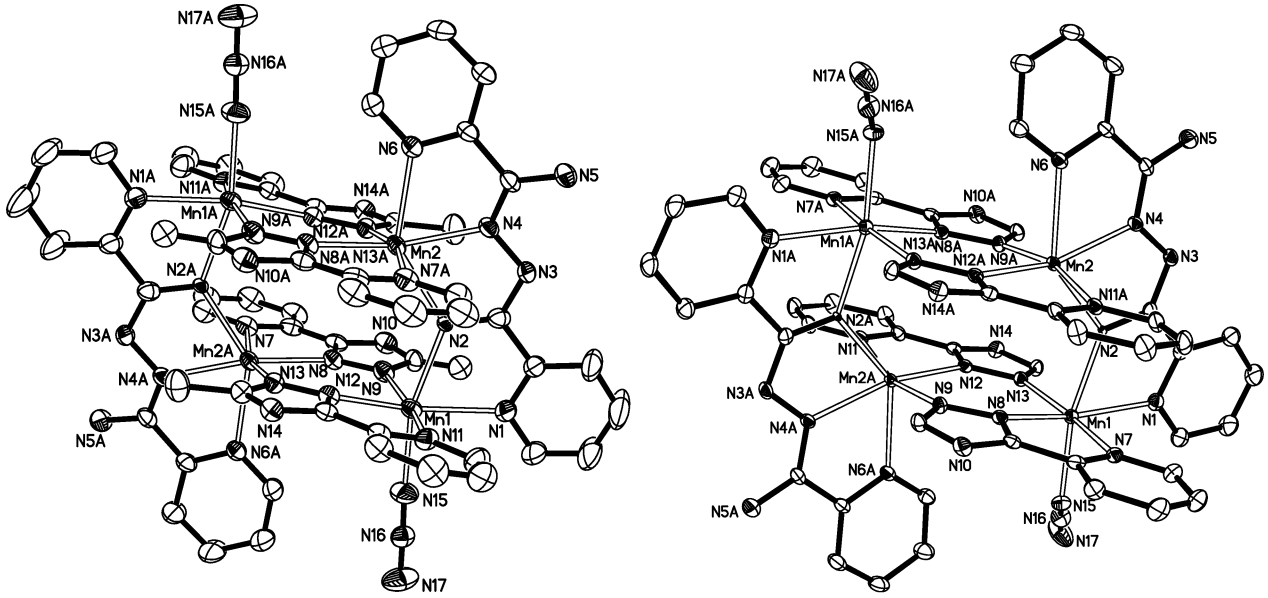

Figure 4. Perspective views of the tetranuclear structures in **5** (a) and **6** (b) (thermal ellipsoids, 30%). Selected interatomic distances (Å) and bond angles (deg) for **5**: Mn1−N2 2.226(5), Mn2−N2 2.234(4), Mn2−N4 2.187(5), C6−N2 1.283(6), C6−N3 1.302(9), C7−N4 1.297(8), C7−N5 1.332(7), Mn1···Mn2 4.02, Mn1···Mn2a 4.32; ∠Mn1−N2−Mn2 128.6(1). Selected interatomic distances (Å) and bond angles (deg) for **6**: Mn1−N2 2.180(3), Mn2−N2 2.206(3), Mn2−N4 2.185(3), C6−N2 1.299(5), C6−N3 1.309(5), C7−N4 1.297(5), C7−N5 1.326(5), Mn1···Mn2 3.91, Mn1···Mn2a 4.28; ∠Mn1−N2−Mn2 125.8(1).

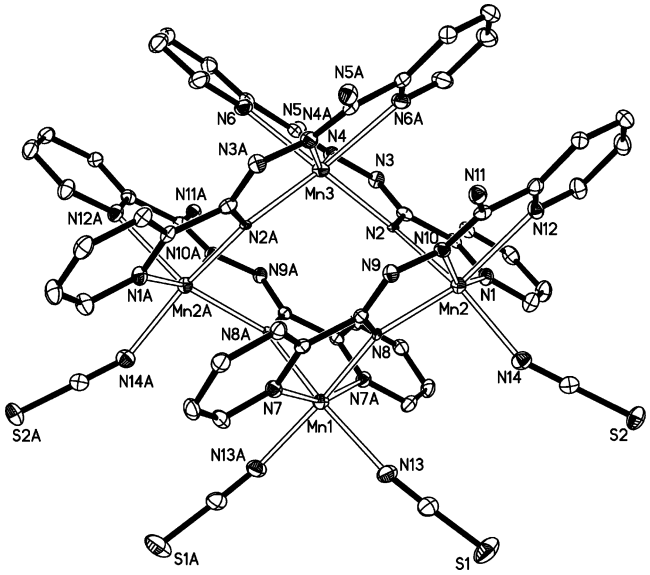

Figure 5. ORTEP drawing of the tetranuclear **7** (thermal ellipsoids, 30%; A, $-x$, y, $^1/_2 - z$). Selected interatomic distances (Å) and bond angles (deg): Mn1−N8 2.175(3), Mn2−N8 2.229(4), Mn2−N2 2.195(3), Mn3−N2 2.224(4), Mn2−N10 2.146(3), Mn3−N4 2.147(3), C6−N2 1.308(6), C6−N3 1.283(6), C7−N4 1.292(6), C7−N5 1.339(7), C18−N8 1.301(6), C18−N9 1.299(6), C19−N10 1.297(6), C19−N11 1.338(6), Mn1···Mn2 3.99, Mn2···Mn3 3.98; ∠Mn1−N8−Mn2 130.1(1), ∠Mn2−N2−Mn3 128.8(1).

pt, while thiocyanate may promote the crystallization of **7**, hence inhibiting the formation of mpt.

As depicted in Figure 5, there are three crystallographically independent Mn^{II} ions, four H_3bpa, and four SCN^- ligands in **7**. Each of the four H_3bpa ligands acts in a pentadentate mode to bind two Mn^{II} ions into two five-membered chelate rings, resulting in a regular [2 × 2] tetranuclear gridlike structure with the metal−metal separations at ca. 3.99 Å and Mn−N−Mn angles at 130.1(1) and 128.8(1)°. In the tetranuclear core, the Mn3 ion is ligated by two tridentate sites of two H_3bpa ligands, while Mn1 is coordinated to two bidentate sites of two H_3bpa ligands and Mn2 binds a bidentate site and a tridentate site of two H_3bpa ligands. Both Mn1 and Mn2 ions are further coordinated by SCN ligands into octahedral geometries. To the best of our knowledge, [2 × 2] grid Mn^{II} complexes are very rare,[38,39] and no neutral [2 × 2] Mn^{II} grid with imino bridges has been reported so far.

Because the H_4bpa intermediate was excluded in the "one-pot" synthesis of 4-amino-3,5-disubstituted 1,2,4-triazole from the reaction of organonitrile with hydrazine hydrate,[26] the successful isolation of H_3bpa in this work indicates that different reaction mechanisms may be involved in the presence and absence of metal ions under solvothermal conditions. So far, three organic species, including *cis*- and *trans*-bpt as well as H_3bpa, have been trapped and isolated from the reaction of 2-cyanopyridine and hydrazine hydrate in the presence of metal ions. From the above observations, the possible mechanisms can be proposed (Scheme 5). Theoretically, two tautomers, 2-pyC(NH_2)═NNH_2 (**A1**) and 2-pyC(═NH)$NHNH_2$ (**A2**), coexist in a solution, and the chelation to a metal center results in stabilization of each tautomer and may further delocalize the π electron density of the imino bond and enhance the nucleophilic reactivity

(38) (a) Murray, K. S. *Adv. Inorg. Chem.* **1995**, *43*, 261−356. (b) Hu, T.-L.; Li, J.-R.; Liu, C.-S.; Shi, X.-S.; Zhou, J.-N.; Bu, X.-H.; Ribas, J. *Inorg. Chem.* **2006**, *45*, 163−173.

(39) (a) Thompson, L. K.; Waldmann, O.; Xu, Z.-Q. *Coord. Chem. Rev.* **2005**, *249*, 2677−2690. (b) Thompson, L. K.; Matthews, C. J.; Zhao, L.; Xu, Z.; Miller, D. O.; Wilson, C.; Leech, M. A.; Howard, J. A. K.; Heath, S. L.; Whittaker, A. G.; Winpenny, R. E. P. *J. Solid State Chem.* **2001**, *159*, 308−320.

Scheme 5. Proposed Mechanisms for the Reaction of 2-Cyanopyridine and Hydrazine Hydrate in the Presence of Metal Ions

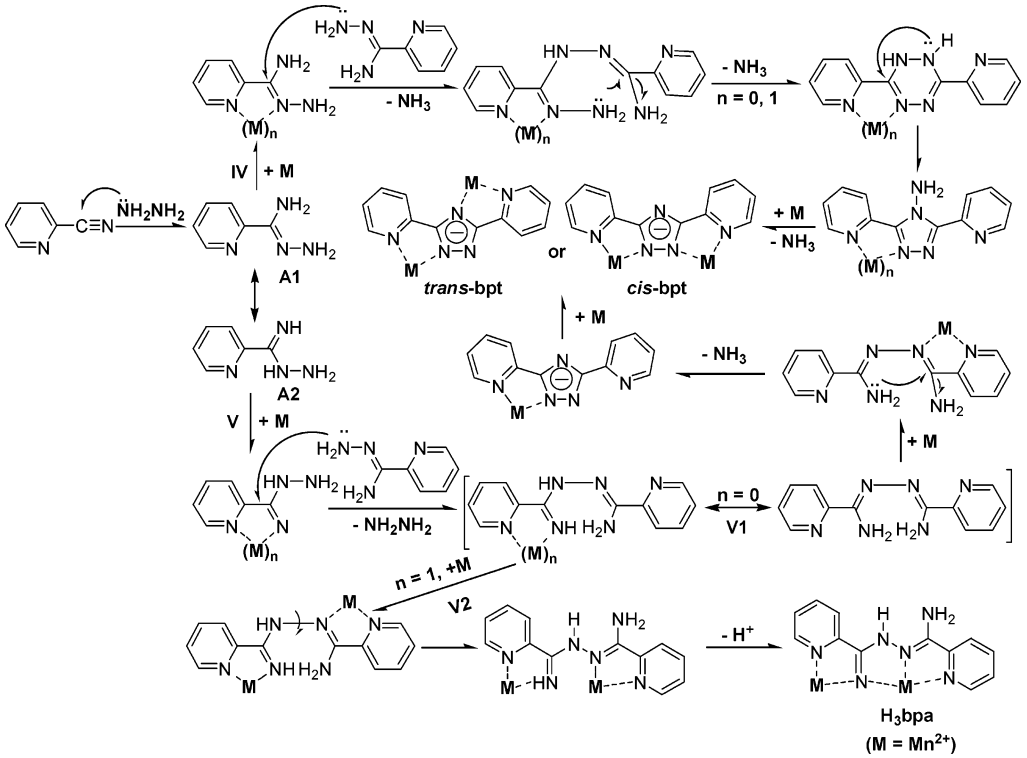

of the C atom.[13] Obviously, the free and coordinated precursors also coexist in the reaction solution as a result of chemical equilibria, in which one may dominant depending on the reaction conditions. First, both metal-containing tautomers coexist and two paths (IV and V) may be involved in the reaction processes. In path IV, the tautomer **A1** may bind to a metal ion in the form of an amidrazone complex, which is nucleophilically attacked on the activated imino C atom by the end amino of another 2-pa. Then, the reaction proceeds via two steps of deamination to give a six-membered-ring precursor of 3,6-bis(substituted) 1,2-dihydro-1,2,4,5-tetrazine and rearrangement into a 4-amino-1,2,4-triazole complex. Finally, the cis product is afforded when the metal binding occurs before deamination of 4-amino-1,2,4-triazole, or both the cis and trans products result if metal coordination takes place after deamination. In the current case, deamination occurs under excessive base and high temperature as well as metal assistance,[40] being different from the general method of deamination via reductive diazotization. In path V, the tautomer **A2** stabilized by a metal ion is nucleophilically attacked by the end amino of another 2-pa, giving rise to a tautomer of H_4bpa upon elimination of a molecule hydrazine. H_4bpa further ligates a metal ion, rotates, and deprotonates into the cis product of H_3bpa in the presence of excessive basic hydrazine (**V2**). On the other hand, the free 2-pa can condense into H_4bpa, which then chelates to a metal ion to activate the imino C atom for more facile attack by another amino group, followed by cycloconsendation and deamination to furnish the final product 1,2,4-triazolate (**V1**).

It should also be noted that only crystalline products were collected; the reported yields in this work should be lower than the practical yields. Even so, most of the crystalline products were obtained in considerable yields.

Magnetic Properties. All compounds **5**−**7** have square or parallelogram tetranuclear structures, respectively, and those of **5** and **6** are very similar. Therefore, only the magnetic properties of **5** and **7** were measured. The magnetic susceptibility of **7** has been measured in the temperature range of 2−320 K at an applied field of 1000 Oe, and the plots of χ_M and its reciprocal $1/\chi_M$ vs T are shown in Figure 6. When the sample is cooled from 320 K, χ_M (0.066 emu mol^{-1}) exhibits an increase as the temperature is decreased with a sharp peak at 19 K (0.3067 emu mol^{-1}) and then decreases to 0.207 emu mol^{-1} at 2 K. The temperature dependence of magnetic susceptibilities above 30 K obeys the Curie−Weiss law $\chi_M = C/(T - \theta)$ with a Weiss constant $\theta = -59.04$ K and a Curie constant $C = 24.76$ cm^3 mol^{-1} K, indicating intramolecular antiferromagnetic coupling between the metal centers.

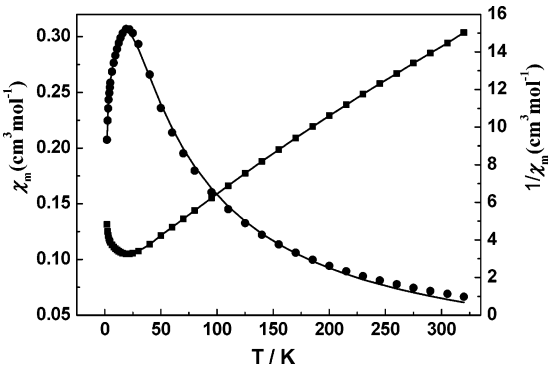

Figure 6. Temperature dependence of χ_M (●) and $1/\chi_M$ (■) for **7**, with the solid lines representing the best fits.

(40) Yang, G.-F.; Yang, H.-Z. *Chin. J. Chem.* **2000**, *18*, 425−427.

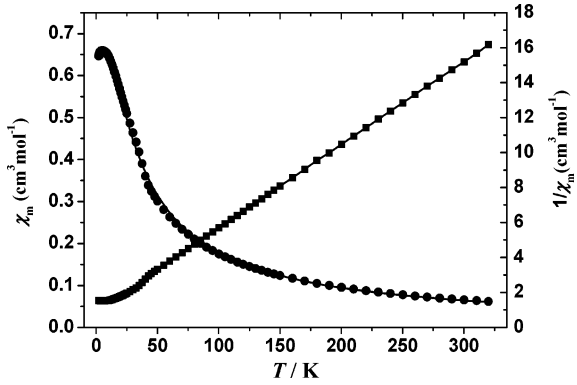

Figure 7. Temperature dependence of χ_M (●) and $1/\chi_M$ (■) for **5**, with the solid lines representing the best fits.

Because the magnetic coupling between the Mn^{II} ions in **7** are mainly operated through the μ-imino groups, the cluster Hamiltonian for a regular [2 × 2] grid Mn^{II}_4 can be written as follows:

$$\hat{H}_{ex} = -2J_1(\hat{S}_1\hat{S}_2 + \hat{S}_3\hat{S}_4) - 2J_2(\hat{S}_2\hat{S}_3 + \hat{S}_4\hat{S}_1) \qquad (1)$$

where J_1 is defined as the exchange along the vertical sides and J_2 as that along the horizontal sides of the square. Because the metal distances (3.99 Å) and angles of Mn−N−Mn [128.8(1) and 130.1(1)°] are almost the same, respectively, a simple case can be considered, in which $S_{1-4} = {}^5/_2$, and $J_1 = J_2$. Using the Kambe vector coupling scheme,[41] a total of 146 energy states are derived (Figure S9 in the Supporting Information). The best fitting of the experimental χ_M data to eq 3 (see the Supporting Information) gives the following parameters: $g = 2.24$, $J = -1.22$ cm^{-1}, $zJ' = -0.48$ cm^{-1}, and $R = 1.7 \times 10^{-4}$. The negative J value confirms the intramolecular antiferromagnetic coupling. The results are comparable to that reported for a Mn^{II}_4 grid ($J = -2.77$ cm^{-1}) connected via alkoxide O atoms with Mn−O−Mn angles in the range 127.9−129.3° and Mn···Mn separations in the range 3.91−3.97 Å.[39]

5 shows a similar profile of χ_M in the temperature range of 2−320 K (Figure 7), indicative of intramolecular antiferromagnetic exchange between the metal centers. χ_M (0.062 emu mol^{-1} at 320 K) exhibits an increase as the temperature is decreased, reaching a peak at 5 K (0.660 emu mol^{-1}), and then decreases to 0.646 emu mol^{-1} at 2 K. The temperature dependence of magnetic susceptibilities above 20 K obeys the Curie−Weiss law $\chi_M = C/(T - \theta)$ with $\theta = -17.7$ K and $C = 20.83$ cm^3 mol^{-1} K. The variable-temperature magnetic data can be fitted to an appropriate exchange expression derived from a spin Hamiltonian as follows:

$$\hat{H}_{ex} = -2J_1(\hat{S}_1\hat{S}_2 + \hat{S}_3\hat{S}_4) - 2J_2\hat{S}_{12}\hat{S}_{34} \qquad (2)$$

This model involves two pairwise exchange interaction constants, J_1 and J_2, between the Mn···Mn interactions. The best fitting of the experimental magnetic data of χ_M to eq 2 gives the following two sets of parameters: $g = 2.14$, $J_1 = -1.00$ cm^{-1}, $J_2 = -0.203$ cm^{-1}, and $R = 2.84 \times 10^{-4}$ and $g = 2.14$, $J_1 = -0.216$ cm^{-1}, $J_2 = -0.677$ cm^{-1}, and $R = 6.48 \times 10^{-4}$, where $R = \sum[(\chi_M)_{obsd} - (\chi_M)_{calcd}]^2/\sum[(\chi_M)_{obsd}]$.[2] Only the data above 5 K were employed to avoid those effects that show up at low temperature (primarily intermolecular interactions and zero-field splitting) but are not taken into account in the theoretical model. The two negative J values are consistent with the structure having one Mn−N−Mn and two Mn−N−N−Mn bridges for transmitting intramolecular antiferromagnetic coupling. Compared with the J value (−1.22 cm^{-1}) for **7**, the former set of fitting data is reasonable and is shown in Figure 7.

Conclusion

The facile and effective one-pot solvothermal syntheses of 3,5-disubstituted 1,2,4-triazoles through cyclocondensations of organonitriles with hydrazine hydrate in the absence/presence of metal salts have been established. By control of the solvothermal conditions and/or the addition of counterions, different intermediates and final products were derived from variable organonitriles.

The results show that, after the initial formation of 2-pyridylamidrazone from organonitriles and hydrazine, two reaction paths are involved in the formation of the 1,2,4-triazoles: via the formation of 3,6-bis(2-pyridyl)-1,2-dihydro-1,2,4,5-tetrazine and H_4bpa as the intermediates. In the absence of metal ions, the first path is dominant, whereas in the presence of metal ions, the latter path may be dominant. In the latter path, the binding of metal ions to the intermediates can stabilize the tautomers, enhance the nucleophilic reactivity of the imino C atom, and inhibit the tautomerization, hence leading to the formation of 1,2,4-triazolates as well as the H_4bpa intermediate. The first in situ solvothermal cyclocondensation reactions of 2-pyridylamidrazone and carboxylate into asymmetric 3,5-disubstituted 1,2,4-triazolates, concomitant with the formation of a deprotonated H_4bpa intermediate, have been observed. Among the crystalline metal complexes, **5**−**7** are all neutral tetranuclear Mn^{II} complexes. Moreover, **7** is the first example of a neutral [2 × 2] Mn^{II} grid structure, and both **5** and **7** exhibit antiferromagnetic interactions.

Acknowledgment. The authors thank Ai-Ping Sun for her help in this work and are indebted to the reviewers for their kind suggestions. This work was supported by the National Natural Science Foundation of China (Grants 20531070 and 20371052) and the Scientific and Technological Department of Guangdong Province (Grant 04205405).

Supporting Information Available: Crystallographic data in CIF format, and additional plots and data for the complexes in PDF format. This material is available free of charge via the Internet at http://pubs.acs.org.

IC061303I

(41) Kambe, K. *J. Phys. Soc. Jpn.* **1950**, *5*, 48−61.